Synthesis and characterization of partially biodegradable and thermosensitive hydrogel

XIAN-ZHENG ZHANG, GUO-MING SUN, DA-QING WU, CHIH-CHANG CHU*
Department of Textiles and Apparel and Biomedical Engineering Program, Cornell University, Ithaca, New York 14853-4401, USA
E-mail: cc62@cornell.edu

A partially biodegradable and thermosensitive hybrid hydrogel network (DAN series) based on dextran-allylisocyanate (Dex-AI) and poly(N-isopropylacrylamide) (PNIPAAm) was synthesized via UV photocrosslinking. These hybrid hydrogels were characterized in terms of their chemical structure, thermal, mechanical, morphological and temperature-induced swelling properties. The effect of the composition ratio of Dex-AI to PNIPAAm on such properties were examined. The differential scanning calorimetry data show that this Dex-AI/PNIPAAm hybrid network has an increased lower critical solution temperature (LCST) and glass transition temperature (T_g) with an increase in the Dex-AI content. The interior morphology of these hybrid hydrogels revealed a decreased porous microstructure with an increase in the Dex-AI content in the hybrid network. Furthermore, if the Dex-AI composition became too high, a distinctive network structure with two different microporous structures appeared. The mechanical properties of these hybrid hydrogels also increased with an increase in the Dex-AI content. The temperature dependence of the swelling ratio, the deswelling kinetics as well as the reswelling kinetics was also characterized by gravimetric method. When comparing with a normal PNIPAAm hydrogel, these Dex-AI/PNIPAAm hybrid networks, due to the presence of Dex-AI moiety, also show improved temperature-induced intelligent properties, such as the faster and controllable response dynamics, which may find promising applications in a wide variety of fields, such as biomedical and bioengineering fields.

Introduction

Intelligent hydrogels have been the subject of extensive research and development since last decade because their volume changes could be triggered by different external stimuli, such as temperature, electric fields, antigen and radiation forces, to name a few. Among the intelligent hydrogels, thermosensitive poly(N-isopropylacrylamide) (PNIPAAm) hydrogel is one of the most extensively studied. PNIPAAm has a lower critical solution temperature (LCST) or transition temperature (T_{tr}) at $\sim 33\,^{\circ}C$ in aqueous solution, and exhibits a thermo-reversible abrupt changes in volume as the external temperature cycles above and below this critical temperature [1–3].

The traditional thermosensitive PNIPAAm-based intelligent hydrogel is usually formed through the reactions of NIPAAm monomers and commercial cross-linking agents, such as N,N′-methylenebisacrylamide, which have two or more double bonds. The resulting hydrogels are non-biodegradable. However, for biomedical application, the biodegradability of the biomaterial is importance due to the absence of a chronic foreign-body reaction after serving its function. In addition, the biodegradation of an implant made from biodegradable biomaterials would eliminate the need for extra surgical procedures to remove the implant from the patient after the implant is no longer needed.

One of the pioneers in the research and development of biodegradable intelligent hydrogels is from the Kim research group (see Jeong *et al.* [4–6]). They proposed a thermosensitive partially biodegradable hydrogel system, and suggested that extensive research and development effort in this area would be beneficial for their potentially promising applications. Kim *et al.*'s thermosensitive biodegradable hydrogels consist of blocks of polymers, such as poly(ethylene oxide) (as non-biodegradable component) and poly(L-lactic acid) (as biodegradable component) etc., and were generated from the reversible sol-to-gel transitions through the reversible physical crosslinking, such as coil-to-helix transition and hydrophobic association, etc., of the aqueous solutions of the copolymers. Due to the existence of the critical gel concentration (CGC), which is inversely related to the molecular weight of the polymer used, sol–gel phase transition occurred around the CGC and the copolymer system acquired thermosensitive property.

*Author to whom all correspondence should be addressed.

In addition to above reported reversible physical crosslinking approach for preparing thermosensitive partially biodegradable hydrogels, a more general approach based on chemical crosslinking for preparing biodegradable and thermosensitive hydrogels continues to be highly desirable. Kumashiro *et al*. [7] recently reported a temperature sensitive polysaccharide which was based on the grafting of a temperature sensitive copolymer [poly(NIPAAm-co-N,N-dimethylacrylamide] (co-polyNIPAAm-DMAAm) onto dextran precursor followed by chemical crosslinking of the grafted dextran precursor with 1,6-hexamethylenediamine crosslinker. They found that, at a temperature below LCST, the extent of enzymatic biodegradation of dextran hydrogel grafted with temperature-sensitive NIPAAm-DMAAm copolymer was reduced as the grafted copolymer length increased; this graft-length dependent enzymatic biodegradation of grafted dextran, however, was not observed at a temperature above the LCST of the grafted segments.

Dextran is a biodegradable polysaccharide and is composed of α-1,6-linked D-glucopyranose residues. Dextran is susceptible to enzymatic digestion in human body and has been used in mediating gene transfection [8]. Dextran-based hydrogels have been extensively studied as the carriers for the delivery of pharmaceutically active drugs [9–13]. Dextran has chemically active functional groups (i.e., –OH group) that can be modified to provide crosslinking sites for the formulation of dextran-based hydrogels [14].

In this study, we reported a different approach to impart temperature stimulating capability to polysaccharides like dextran. Instead of grafting the temperature sensitive segment onto dextran backbone as Kumashiro *et al*. did, we photocrosslinked modified dextran precursor (dextran-allylisocyanate, Dex-AI) with the temperature sensitive PNIPAAm segments by long wavelength UV, and the resulting PNIPAAm/Dex-AI hybrid network would have two types of macromolecules that crosslinked together, Dex-AI and PNIPAAm macromers. Within this hybrid network, there are two types of crosslinking bonds, PNIPAAm to Dex-AI and Dex-AI to Dex-AI. This new hybrid network would be expected to have the biodegradable property from the dextran segment as well as the thermosensitive capability as the PNIPAAm segments would undergo a coil (soluble)-globule (insoluble) transition as external temperature cycles across LCST [15–18]. The effect of the different composition ratio of Dex-AI to PNIPAAm on the thermosensitivity of the resulting hybrid network was examined by differential scanning calorimetry (DSC) for determining their LCST, by scanning electron microscopy (SEM) to investigate the interior morphology as well as by temperature dependence of equilibrium swelling ratio, the deswelling and swelling kinetics of the hybrid network.

Experimental section

Materials

Dextran (Dex) of MW 43 000 and allyl isocyanate (AI) were purchased from Sigma Chemical Company (St. Louis, MO, USA). Dimethyl sulfoxide (DMSO), dibutyltin dilaurate (DBTDL), dimethyl formamide (DMF), 2,2-dimethoxy-2-phenyl acetophenone (DMPAP),N-isopropylacrylamide (NIPAAm) and other chemicals were purchased from Aldrich Chemical Company (Milwaukee, WI, USA).

Synthesis of the dextran-allyl isocyanate (Dex-AI)

Dextran-based precursor (Dex-AI) was synthesized and characterized according to our previously published paper [13]. Briefly, dextran reacted with allyl isocyanate (AI) in the presence of DBTDL catalyst first. At room temperature (22 °C), dry dextran (e.g. 5 g) was dissolved in anhydrous DMSO (60 ml) under nitrogen. DBTDL catalyst (1.83 ml) was injected into the solution at room temperature dropwise, and AI (2.73 ml) was subsequently added dropwise. The reaction mixture was stirred at a predetermined temperature (22 °C) and time (6 h). The resulting polymer was precipitated in excessive cold isopropanol. It was further purified by dissolution and precipitation with DMSO and isopropanol, respectively. The Dex-AI precursor was dried at room temperature under vacuum for a week and stored in a cold dark place before characterization and hydrogel fabrication. The Dex-AI precursor of degree of substitution (DS, the number of AI groups per 100 anhydroglucose units) 2.78 was synthesized and used in this study.

Preparation of the Dex-AI/PNIPAAm hydrogels

Different weight ratios of Dex-AI and NIPAAm were dissolved in pure DMF to make 10% (w/v) concentration solutions. The photo initiator, DMPAP, was added into the solution of the precursors. This transparent solution was irradiated by a portable long-wavelength UV lamp (365 nm, 8 W) for 22 h at room temperature to photocrosslink Dex-AI precursor with NIPAAm as well as photopolymerization of the NIPAAm precursors. The resultant hybrid networks were then purified with distilled water at room temperature for at least 48 h and the water was refreshed every few hours during this treatment. After this purification, the hybrid networks were cut into small discs (12 mm in diameter and 2 mm in thickness) carefully for characterizing their temperature-sensitive capability. The feed compositions ratios of the precursors and other reactants are listed in Table 1. The hybrid network prepared here is labeled as DAN hybrid series (D = Dex; A = AI and N = NIPAAm).

FT-IR analyses of Dex-AI/PNIPAAm Networks

The hybrid network samples were analyzed by a Nicolet Magna 560 FTIR spectrophotometer (Madison, WI) in the region of 3800–1000 cm^{-1}. Prior to the measurement, the network samples were vacuum dried overnight till no weight change. The dried hybrid samples were pressed into the powder, mixed with 10 times as much KBr powder, and then compressed to make a pellet for FTIR characterization.

TABLE I Feed compositions of the partially biodegradable, temperature sensitive Dex-AI/PNIPAAm (DAN) hydrogels[a]

	Sample ID				
	DAN1	DAN2	DAN3	DAN4	DAN5
NIPAAm (mg)	160	130	100	70	40
Dex-AI[b] (mg)	40	70	100	130	160
Photo-initiator (mg)	10.0	10.0	10.0	10.0	10.0
Conversion (%)[c]	—[d]	47.2	63.2	73.8	68.2

[a]All reactions were carried out for 22 h at room temperature in pure DMF.
[b]DS = 2.78 (DS means degree of the substitution or the number of AI groups per 100 anhydroglucose units).
[c]Weight percentage of the synthesized hydrogel from the monomers.
[d]Hydrogel did not form.

Mechanical properties

The mechanical properties of the Dex-AI/PNIPAAm network samples were measured by an Instron tester model 1122 (Instron Corporation) at 22 °C (50% humidity) with a compression load cell having a full-scale range of 2.0 KN. All the samples were immersed in water at room temperature for five days to reach the swollen state, the swollen hydrogel was then placed on the top plate of a compression load cell and compressed by a cylindrical shaped metal rod probe (diameter 6 mm) at a constant crosshead speed of 0.5 mm/min until fragmentation of the hydrogel occurred. The thickness of the hydrogel was evaluated using a compressometer (Frazier Instruments, Hagerstown, MD). Initial compression modulus was calculated from the initial slope of the stress–strain curve and was used to represent the hydrogel mechanical property.

Thermal property of Dex-AI/PNIPAAm networks

LCST measurement

The thermal behavior or LCST of the Dex-AI/PNIPAAm network samples was determined by a differential scanning calorimeter (TA 2920 Modulated DSC, TA instruments, USA). All network samples were immersed in distilled water at room temperature to form hydrogels and they were allowed to swell to reach their equilibrium state before the LCST measurement. For each DSC measurement, about 10 mg equilibrium swollen sample was placed inside a hermetic aluminum pan, and then sealed tightly by a hermitic aluminum lid. The thermal analyses were performed from 25 to 55 °C on the swollen hydrogel sample at a heating rate 3 °C/min under dry nitrogen. The onset temperature of the endotherm was referred as the critical transition temperature or LCST.

Glass transition temperature

Glass transition temperature (T_g) of the vacuum dried hybrid networks was also investigated by DSC (TA 2920 Modulated DSC, TA Instruments, USA). The vacuum dried Dex-AI/PNIPAAm sample was first heated from room temperature to 200 °C at a heating rate of 20 °C/min. Then the sample was immediately cooled to 0 °C at a cooling rate of 10 °C/min. This conditionally cooled sample was then heated again from 0 °C to 200 °C at a heating rate of 20 °C/min. The glass transition was determined from the trace of this second DSC run based on the criterion of T_g at $\Delta C_p/2$.

Interior morphology

The hydrogel network samples were first equilibrated in distilled water at room temperature for 48 h and the equilibrated hydrogel samples were quickly frozen in liquid nitrogen and further freeze-dried in a Virtis Freeze Drier (Gardiner, NY, USA) under vacuum at −42 °C for at least three days until all the solvent was sublimed. Then, the freeze-dried hydrogel was fractured carefully and the cross-section or interior morphology of the hydrogel was studied by using a scanning electron microscope (Hitachi S4500 SEM, Mountain View, CA). Before SEM observation, hydrogel specimens were fixed on aluminum stubs and coated with gold for 40 s.

Swelling ratio, its temperature dependence, swelling and deswelling kinetics

Swelling ratio at room temperature

All the hydrogel samples were immersed and swollen in distilled water at room temperature for at least 24 h to reach their equilibrium swelling ratios before gravimetric measurement. After the removal from the immersion glasswares, the excess water on the swollen hydrogel surface was removed by wet filter paper. The average values among three measurements were taken for each sample and the equilibrium-swelling ratio at room temperature, SR_{eq}, was calculated as follows:

$$SR_{eq} = W_s/W_d \quad (1)$$

where W_s is the weight of water in the equilibrium swollen hydrogel (wet weight – dry weight) and W_d is the initial dry hydrogel weight at time 0.

Swelling kinetics at room temperature

The swollen hydrogel samples were first immersed in hot water (48 °C) for 6 h, and the partly shrunk hydrogels were further dried in vacuum oven at 55 °C overnight until the hydrogel reached constant weight. The dried samples were then placed in distilled water at 22 °C and removed from water at regular time intervals. After wiping off the water on the surfaces of the samples with moistened filter papers, the weights of hydrogels were recorded. The water uptake at time t is defined as follows:

$$[\text{Water uptake}]_t = [(W_t - W_d)/W_s] \times 100 \quad (2)$$

where, W_t is the weight of the wet hydrogel at time t and 22 °C, and the other symbols are the same as above.

Temperature dependence of the swelling ratio

For the temperature dependent swelling ratio study, hydrogels were equilibrated in distilled water at a

temperature ranging from 22 to 65 °C, which cover the expected range of LCSTs of the Dex-AI/PNIPAAm hybrid hydrogels. The samples were allowed to swell in distilled water for at least 24 h at each predetermined temperature controlled up to $\pm$ 0.1 °C by a thermostated water bath (Grant Precision Stirred Bath, Grant Instruments Ltd, Cambridge, England). After 24 h immersion in distilled water at a predetermined temperature, the hydrogels were removed, and excess water on the surface of the wet hydrogel was blotted by wet filter papers and then weighted until constant weight was reached. After this weight measurement, the hydrogel was re-equilibrated in distilled water at another predetermined temperature and its wet weight was determined thereafter. The dry weight of each sample was determined after drying to constant weight under vacuum at 55 °C for overnight. Swelling ratio at each temperature was then calculated according to Equation 1 above. An average value of three measurements was recorded for each sample.

Deswelling kinetics

The deswelling kinetics of the Dex-AI/PNIPAAm hydrogels was measured gravimetrically at 48 °C. This temperature was well above the LCST of the hybrid hydrogels so that dramatic shrinkage in volume or discontinuous phase separation could be attained within a short time. The hydrogel samples were first immersed in distilled water at an ambient temperature until equilibrium. The equilibrated hydrogel samples were then quickly transferred into a water bath at a temperature of 48 °C. At predetermined time intervals, the samples were taken out from the hot water and weighted after wiping off the excess water on the surface with filter papers. Water retention was defined as follows:

$$[\text{Water retention}]_t = [(W_t - W_d)/W_s] \times 100 \quad (3)$$

where W_t is the weight of the wet hydrogel at time t and 48 °C, W_s is the equilibrium water weight at room temperature and the other is the same as defined above.

Results and discussion

Formation of the Dex-AI/PNIPAAm network

The chemical structures of NIPAAm, dextran and Dex-AI are shown in Fig. 1 and an example of their corresponding hybrid network structure is shown in Fig. 2. The successful incorporation of the AI group into dextran to form Dex-AI precursor is demonstrated by the presence of unsaturated functional groups (> C=C <) as well as urethane linkage in the ally isocyanate group as shown in the FTIR of Dex-AI in Fig. 3. The FTIR data clearly show the typical double-bond absorption bands at 1645 cm^{-1} (band *c* in Fig. 3) for the C=C stretching vibration in Dex-AI, which confirmed that the double bonds were successfully incorporated into the dextran. The strong absorption band at 1720 cm^{-1} (band *a* in Fig. 3) was from the carbonyl stretch band in Dex-AI and the characteristic band at 1540 cm^{-1} (band *d* in Fig. 3) indicated the presence of NH groups of the urethane linkage in dex-AI. While the band at around 1650 cm^{-1} (band *b* in Fig. 3) in the dextran spectrum was due to the presence of a trace amount adsorbed water that was difficult to remove in dextran [13].

During the formation of the DAN hybrid network, the Dex-AI reacted as a precursor as well as a crosslinker since the photocrosslinkable groups (i.e., AI) are located in the anhydroglucose units along dextran backbone. Therefore, there are two types of crosslinking bonds in the Dex-AI/PNIPAAm hybrid network: PNIPAAm to Dex-AI and Dex-AI to Dex-AI.

Table I illustrates that the percentage of conversion (wt %) of the synthesized hybrid network from its precursors increases with an increase in the Dex-AI content from DAN2 (47.2%) to DAN4 (73.8%). However, if the content of Dex-AI moiety becomes too high, the % conversion would be reduced, that is, DAN5 (68.2%). The increase in conversion efficiency is attributed to the increased photocrosslinking level of the resulting hybrid network from the increasing Dex-AI moiety in the precursor composition ratio. But, due to the possible steric hindrance of the Dex-AI, the conversion efficiency would be slightly reduced, if the content of the Dex-AI would be too high as DAN5 sample. DAN1 hybrid network could not be formed and hence would not be discussed for the remaining of this paper.

Attributed to biodegradable nature of the dextran component, this Dex-AI/PNIPAAm hybrid network is partially biodegradable, and the biodegradation behavior and mechanism of the dextran-based hydrogels have been extensively investigated and reported [19–24]. In additional to this inherent biodegradability from dextran component, this hybrid hydrogel is also temperature sensitive due to its thermo-sensitive moiety, NIPAAm.

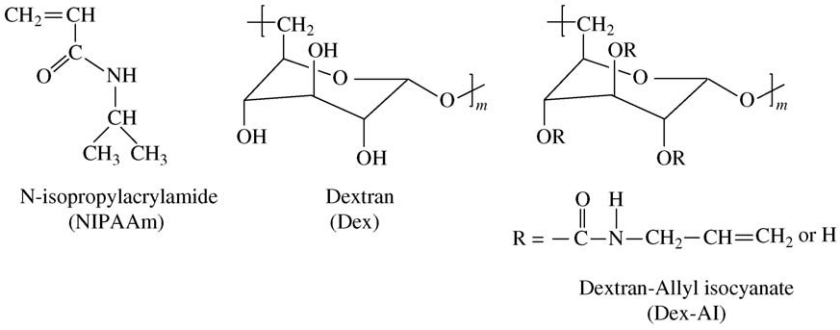

Figure 1 Chemical structure NIPAAm, Dex and Dex-AI.

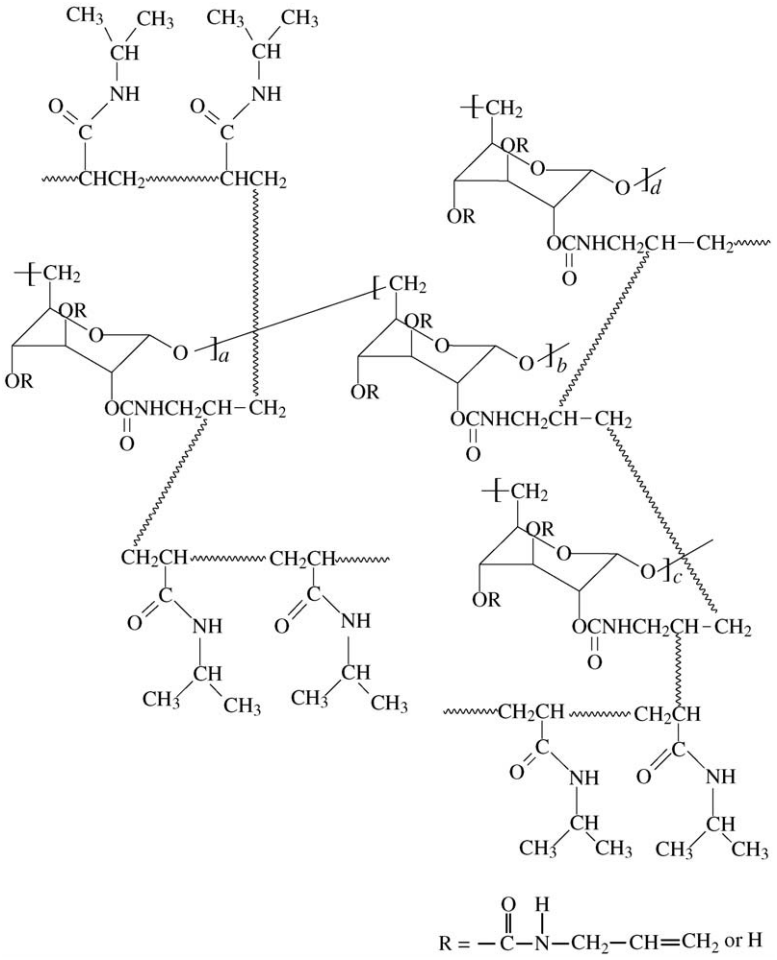

Figure 2 Schematic illustration of the structure of Dex-AI/PNIPAAm hydrogel.

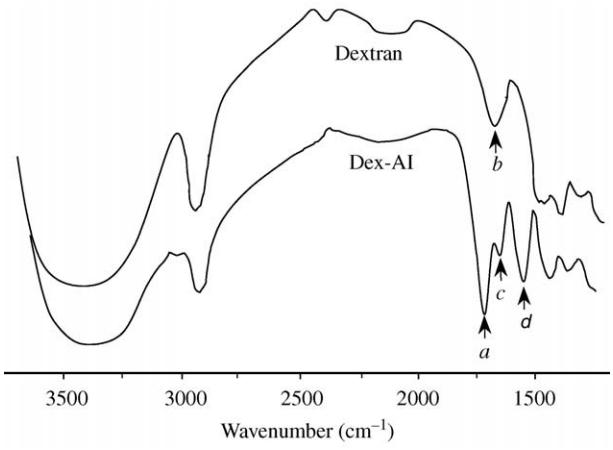

Figure 3 FT-IR spectra of the Dextran and Dex-AI: (a) $\sim 1720\,cm^{-1}$; (b) $\sim 1650\,cm^{-1}$; (c) $\sim 1645\,cm^{-1}$; and (d) $\sim 1542\,cm^{-1}$.

FT-IR spectra of Dex-AI/PNIPAAm network

The FT-IR spectra of the Dex-AI/PNIPAAm hybrid network samples are shown in Fig. 4. The IR spectra of all the DAN samples are generally similar to each other, although the spectrum of each hybrid network shows slight change in band intensity due to different Dex-AI to NIPAAm precursor composition ratio from DAN2 to DAN 5. Each spectrum has a broad band in the range of 3700–3100 cm^{-1}, which is assigned to O–H and N–H stretching vibrations of Dex-AI and PNIPAAm. In the spectra, typical amide I band at $\sim 1645\,cm^{-1}$ (band *b* in Fig. 4) and amide II band at $\sim 1533\,cm^{-1}$ (band *c* in Fig. 4) are evident. A typical band from the stretching of carbonyl groups was also found for Dex-AI at $\sim 1704\,cm^{-1}$ (band *a* in Fig. 4) and as the Dex-AI moiety increased from DAN2 to DAN5, the intensity of this peak increased accordingly, which confirms that more Dex-AI were incorporated into the hybrid network from DAN2 to DAN5.

Mechanical properties of Dex-AI/PNIPAAm network

The initial compression moduli of the swollen Dex-AI/PNIPAAm hydrogels were shown in Fig. 5. The data support and confirm our argument that, with an increase in Dex-AI moiety from DAN2 to DAN5, their mechanical property increased accordingly. For example, the compression modulus of DAN5 (27.7 KPa) was about five times higher than the one of DAN2 (5.4 KPa).

This trend of the increasing mechanical property from DAN2 to DAN5 is easy to understand since an increased Dex-AI moiety greatly increases the crosslinking extent among the corresponding hybrid network due to the fact that the crosslinkable units in Dex-AI are located along the anhydroglucose dextran backbone. In other words, due to the increased crosslinkable units from DAN2 to DAN5, the average chain length between two cross-linking points was shortened and a more compact, regular and rigid network structure would be formed accordingly. This would lead to a higher compression modulus from DAN2 to DAN5 as observed. As described

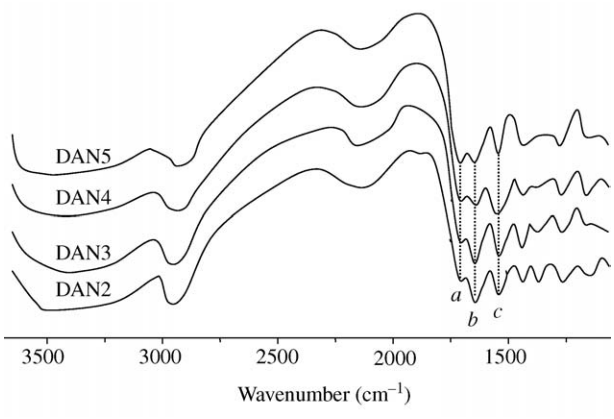

Figure 4 FT-IR spectra of the Dex-AI/PNIPAAm hydrogels (a) $\sim$1704 cm^{-1}; (b) $\sim$1645 cm^{-1}; (c) $\sim$1533 cm^{-1}.

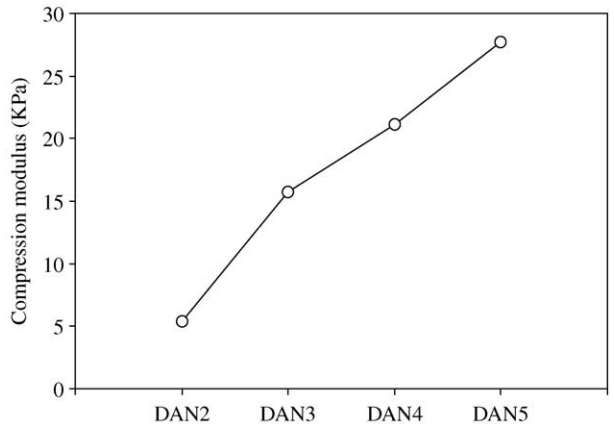

Figure 5 Comparison of the initial compression modulus of the swollen Dex-AI/PNIPAAm hydrogels.

later, the SEM morphology data (shown in Fig. 8) also confirm this argument further.

DSC thermograms of Dex-AI/PNIPAAm network

DSC data of the Dex-AI/PNIPAAm hybrid network over the temperature range from 25 to 55 °C are shown in Fig. 6. The LCST was defined as the onset temperature of the endotherms [25, 26] as shown in Fig. 6. DAN2 $\sim$ 4 clearly exhibit the presence of LCSTs, which increases from DAN2 (35.6 °C) to DAN4 (37.3 °C). When comparing to the LCST of a normal PNIPAAm hydrogel (35 °C) [26] all the DAN hybrids have higher LCST than the 100% PNIPAAm value.

Many factors may affect the LCST of the thermosensitive hydrogel; for example, as Kumashiro *et al*. [7] reported that the chain length of the NIPAAm-DMAAm copolymer rather than the number of copolymer chains that was grafted onto dextran has some effects on LCST of the whole system. The LCST of the NIPAAm-DMAAm copolymer grafted dextran ranged from 40.3 to 42.2 °C.

Generally, it is known that there is a hydrophilic/hydrophobic balance in the PNIPAAm network system and there exist many interactions, such as hydrogen bonding interactions as well as polymer–polymer interactions, which lead to good solubility of the PNIPAAm hydrogel at room temperature (the temperature below its LCST) [27–32]. As the temperature increases to its corresponding LCST, these interactions are destroyed and the hydrophobic interactions among the hydrophobic groups in the PNIPAAm segments would become overwhelm [27, 33, 34]. At this stage, PNIPAAm chains precipitate from the water and the hydrogel structure collapses in volume, that is, a phase separation from the aqueous medium.

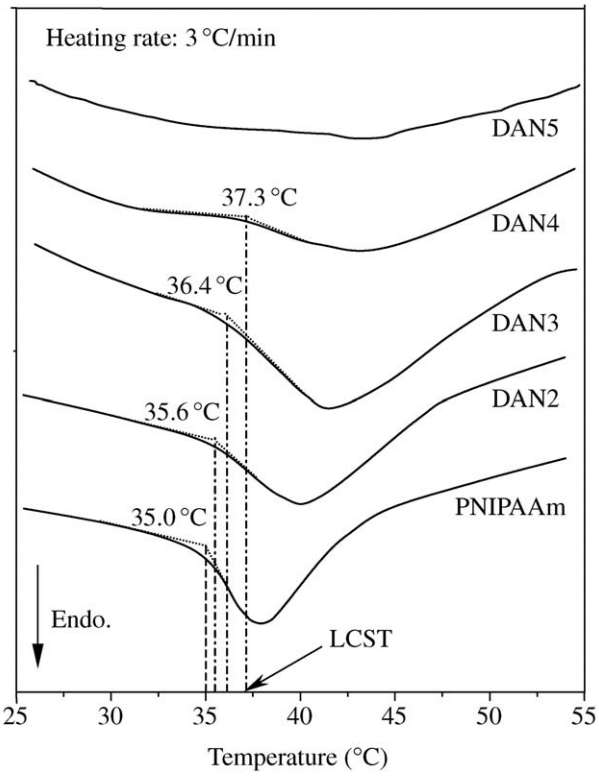

Figure 6 DSC thermograms of the Dex-AI/PNIPAAm hydrogels.

As mentioned above, Dex-AI is used as the precursor as well as the crosslinker during the gelation process. Obviously, with an increase in Dex-AI composition, the resulting hybrid network would have an increased crosslinking level. According to our previously reported findings [35], an increase in crosslinking level should not affect the LCST of the PNIPAAm hydrogel, which is different from what we observed here. Therefore, the observed increase in the LCST ($\Delta T_{LCST} = 2.3$ °C) of the DAN hybrid series with an increase in the Dex-AI component may be attributed to the strengthened inter/intramolecular interactions, such as hydrogen bonds, in these hybrid network systems from DAN2 to DAN4. Such a strengthen of inter/intramolecular interactions is because Dex-AI has many –OH groups that not only would provide more hydrophilicity to the hybrid network but also could facilitate the formation of hydrogen bonds. The resulting three-dimensional Dex-AI/PNIPAAm network structure having more Dex-AI constituent is, therefore, more hydrophilic and compact than a 100% PNIPAAm network prepared from normal crosslinker like N, N′-methylenebisacrylamide. As a result, more energy would be required to break the strengthened inter/intramolecular interaction in the Dex-AI/PNIPAAm network, that is, a high LCST observed. This increasing inter- or/and intramolecular interaction with an increase in the Dex-AI moiety in the hybrid network is also consistent with the observed glass

transition temperature data of the hybrid network described below.

As the Dex-AI component became overwhelm in the Dex-AI/PNIPAAm hybrid network (DAN5), however, no obvious LCST could be found. This indicates that the temperature sensitivity of DAN5 is too weak to measure due to the presence of very small amount of PNIPAAm moiety.

Glass transition temperature of the Dex-AI/PNIPAAm network

Fig. 7 shows the T_g values of the Dex-AI/PNIPAAm network as a function of the composition ratio of the two precursors in the hybrid networks. The T_g data illustrate two important findings: only a single T_g was exhibited for each hybrid network, and T_g falls between the range of 100% PNIPAAm and 100% Dex-AI and increased with an increase in Dex-AI component in the hybrid network, that is, from 137.5 of DAN2 to 168.2 °C of DAN5.

The appearance of a single T_g for each hybrid network indicates the miscibility of the Dex-AI and PNIPAAm segments, that is, no phase separation due to two immiscible components. Both the Dex-AI and NIPPAAm precursors were successfully integrated together without phase separation over the composition ratio range studied. The dependence of T_g on the precursor composition ratio in the hybrid network can be examined first from the T_g of normal pure PNIPAAm hydrogel [36, 37] and pure Dex-AI hydrogel [38]. Generally, the glass transition indicates the initiation of the polymer chains' mobility from the ''frozen glassy'' state. If the interactions among the polymer chains were strong, a higher temperature would be needed to overcome these polymer–polymer interactions for facilitating this mobility of polymer chains. Based on this viewpoint, the observed highest and lowest T_g of the group (Dex-AI network at 179 °C and PNIPAAm network at 131.4 °C) suggests that the polymer–polymer interactions in the Dex-AI network are much stronger than the ones in pure PNIPAAm network. An examination of the chemical structural difference between Dex-AI and PNIPAAm would support the relationship between T_g and level of intermolecular interaction of polymers. The presence of the vast amount of –OH groups in Dex-AI would certainly facilitate far more intermolecular or/and intramolecular interactions than PNIPAAm, and hence a higher T_g for Dex-AI. Therefore, a hybrid network having a higher amount of Dex-AI moiety like DAN4 and 5 would be expected to have a higher T_g than those hybrid networks having a lower amount of Dex-AI like DAN2. Our experimental findings of T_g of the DAN hybrid series exactly support such a theoretical prediction and are also consistent with the LCST data observed.

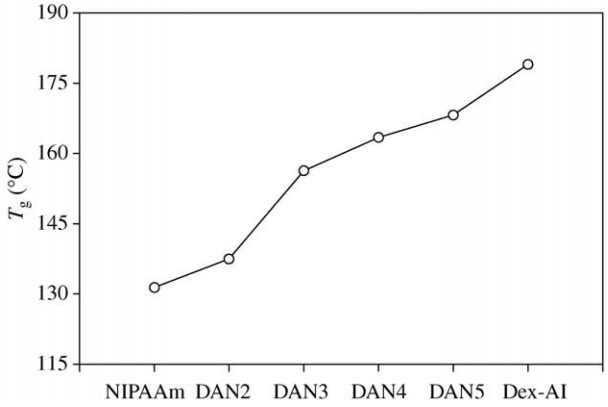

Figure 7 Glass transition temperature (T_g) of the Dex-AI/PNIPAAm hydrogels.

Interior morphology of the Dex-AI/PNIPAAm hybrid hydrogels

The interior morphology of these freeze-dried, swollen hydrogel samples as a function of the precursor composition ratio are shown in Fig. 8. Except DAN5, the Dex-AI/PNIPAAm hybrid hydrogel network became tighter and more compact with an increase in Dex-AI component from DAN2 to DAN4. The average pore size of the DAN2 is the largest and is around 10 μm, while DAN4 has pores significantly smaller than 10 μm. The pore number in the hybrid networks, however, was inversely proportional to the pore size with DAN4 having the largest pore number followed by DAN3 and DAN2. This precursor composition-dependent pore size of the DAN hybrid series can be attributed to a higher level of intermolecular interaction from a higher crosslinking level as the Dex-AI component increases from DAN2 to DAN4, that is, denser and more compact network structure.

DAN5 exhibits an interior morphology vastly different from other DAN samples as shown in Fig. 8. It appears to have two distinctive but interwoven networks – one with loose fishing net structure having larger pores and one with much tighter and smaller pores network locating within the large pores of the loose fishing net (see the enlarged insert of upper right corner of Fig. 8). It is difficult to determine which of the two precursors, Dex-AI or PNIPAAm, is responsible for which of the two distinctive network appearances. Due to the overwhelming Dex-AI content over NIPPAAm in DAN5 (see Table I), we speculate that the larger loose net might be from the Dex-AI precursor that were difficult to crosslink due to the steric hindrance; while the tighter and small pore network may come from the PNIPAAm and Dex-AI. The fishing net like structure appears to be slightly similar to Zhang *et al*. [26] prior study of cold treated PNIPAAm hydrogel. This unusual interior morphology of DAN5 is also responsible for its swelling, deswelling behavior to be described below.

Swelling ratio at room temperature of Dex-AI/PNIPAAm hybrid hydrogels

Fig. 9 shows the dependence of swelling ratios of Dex-AI/PNIPAAm hybrid hydrogels at room temperature on their composition ratio. The data show that the swelling ratio of Dex-AI/PNIPAAm hydrogels at room temperature (below their LCST) decreased with an increase in Dex-AI content (from DAN2 to DAN4) and, then, increased slightly from DAN4 to DAN5. The swelling

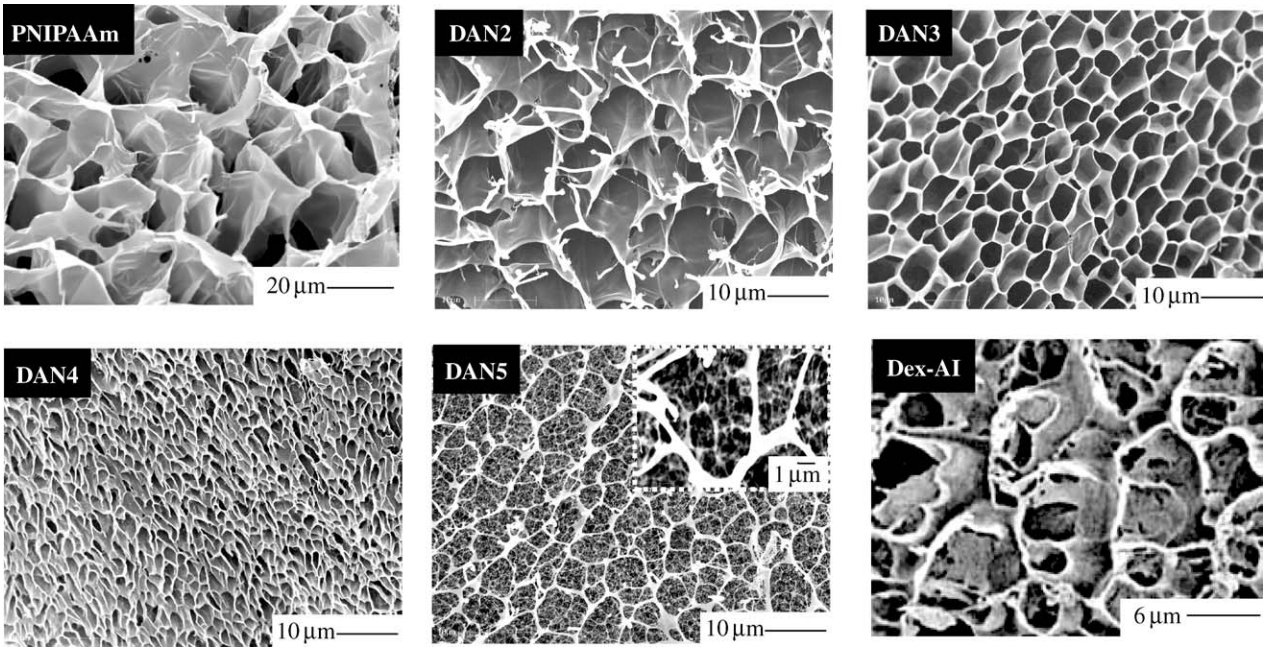

Figure 8 SEM micrographs of the Dex-AI/PNIPAAm hydrogels after two days immersion in water (SEM micrographs of the controls: PNIPAAm hydrogel[26] and Dex-AI hydrogel[9] are from our prior works).

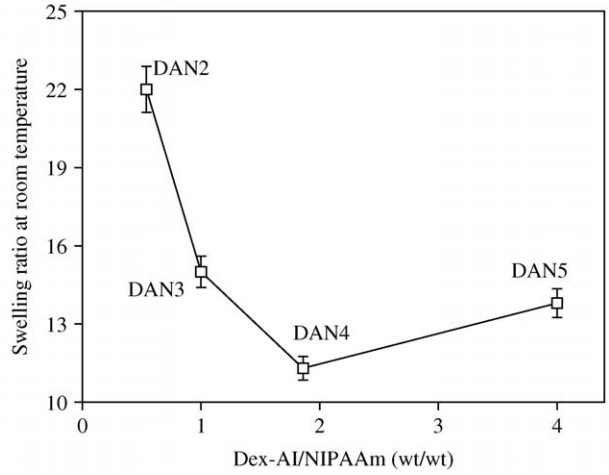

Figure 9 Swelling ratios of the Dex-AI/PNIPAAm hydrogels at room temperature.

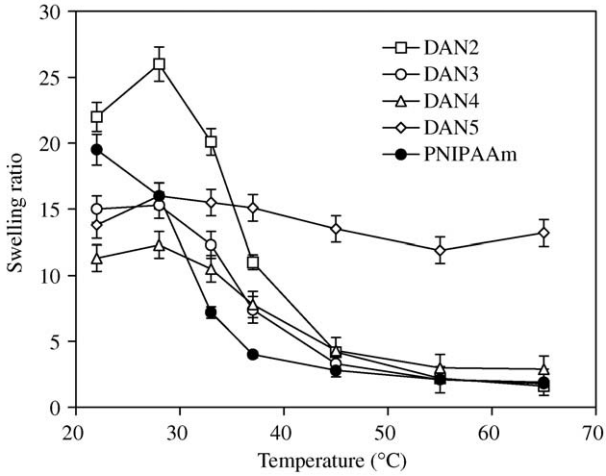

Figure 10 Temperature dependence of swelling ratio of the Dex-AI/PNIPAAm hydrogels in the temperature range from 22 to 65 °C.

ratio was reduced to half of its value as from DAN2 (22) to DAN4 (11.3).

The reduction of swelling ratio at room temperature from DAN2 to DAN4 is consistent with their morphology observed (Fig. 8). As described above, an increase in the content of the Dex-AI component from DAN2 to DAN4 led to a tighter, denser and smaller pore network structure due to a higher crosslinking level of the corresponding hydrogel, that is, a reduction in swollen capacity or water uptake due to the decreased pores volume for retaining the water. However, in the case of DAN5, its swelling ratio at room temperature increased slightly from DAN4, and is believed to be attributed to the presence of the distinctive loose large pore fishing net structure.

Temperature dependence of the swelling ratio of Dex-AI/PNIPAAm hybrid hydrogels

Fig. 10 demonstrates the classical temperature dependence of swelling ratio of Dex-AI/PNIPAAm hydrogel series over a temperature range from 22 to 65 °C, which covers the expected range of LCST of the hybrid hydrogels. The data show that, regardless of the Dex-AI to PNIPAAm composition ratio, all the hybrid hydrogel samples have the classical temperature-regulated swelling as the 100% PNIPAAm hydrogel does. However, the sensitivity to temperature-dependent swelling decreased with an increase in Dex-AI content in the hybrid hydrogels from DAN2 to DAN5. For example, DAN2 had the largest change in swelling ratio ($\Delta SR = SR_{28\,^\circ C} - SR_{45\,^\circ C} = 22$) upon temperature-induced deswelling when the external temperature was increased from 28 to 45 °C, while the corresponding changes in swelling ratio for DAN 3, DAN 4 and DAN5 were much smaller and the ΔSR were around 12, 8 and 2.5, respectively.

Although the Dex-AI/PNIPAAm hybrid hydrogels exhibit the similar temperature-dependent swelling behavior as the 100% PNIPAAm hydrogel does, the initial pattern of the swelling of the hybrid hydrogels at

the temperature few degrees above room temperature but below their LCST is quite different, that is, their swelling ratios increased a little initially (especially DAN2) with an increase in temperature, a characteristic that is not found in the normal PNIPAAm hydrogel. It is probably due to the destruction of hydrogen bond interactions among the hybrid hydrogel. As temperature increased slightly above the room temperature, the driving force for network expansion resulting from the destruction of the hydrogen bonds overwhelmed the driving force for strengthening hydrophobic interactions between the hydrophobic groups. Thus, the networks were slightly expanded as the swelling temperature increased slightly above the room temperature. However, Dex-AI/PNIPAAm hybrid hydrogel networks having a higher Dex-AI composition like DAN3 and 4 did not show such drastic initial network expansion with temperature as DAN2. This might be attributed to the larger amounts of hydrogen bond formation in DNA3 and DAN4 network, which make the destruction of H-bonds more difficult as the temperature increases slightly above room temperature but below their LCST, i.e., not enough thermal energy from the slight increase in temperature to expand network.

Our findings of the effect of hydrophilic Dex-AI component on the initial increasing swelling of Dex-AI/PNIPAAm hybrid hydrogels at the temperature slightly above room temperature but below their LCST are similar to Zhang *et al*. [39] reported study of poly(NIPAAm-co-acrylic acid) hydrogel. In that copolymer system, Zhang *et al*. [39] observed the same phenomenon as our Dex-AI/PNIPAAm hybrid hydrogel: an initial increase in swelling ratio of poly(NIPAAm-co-acrylic acid) hydrogel having a smaller acrylic acid component at a temperature below its LCST and this initial increase in swelling ratio disappeared with a further increase in acrylic acid content in the copolymer hydrogel.

As the swelling temperature increased further, the swelling ratios for all the hybrid hydrogels decreased because the hydrophobic interactions between the hydrophobic groups of the hydrogels became dominant and thus the hydrogel matrices shrank. The level of reduction in swelling ratio of the DAN hybrid series with an increase in temperature to near their LCST (in terms of the magnitude of the negative swelling slope) was the highest for DAN2 and the smallest for DAN5, suggesting that the temperature stimulating capability of PNIPAAm is diluted as the Dex-AI component in the hybrid hydrogels was increased. For DAN5, there was very little reduction in swelling ratio over the whole temperature range.

At the temperatures above LCST, all DAN samples, except DAN5, collapsed to the same level of swelling as 100% PNIPAAm. This is because the intrinsic affinity of PNIPAAm chains in the hybrid hydrogels became dominant due to thermal dissociation of the hydrating water molecules from the polymer chains (cleavage of hydrogen bonds). Consequently, the inherent hydrophobic interactions between isopropyl side chains of PNIPAAm drastically increase, i.e. resulting in the association of hydrophobic polymer chains, and phase separation was observed for the hybrid hydrogels DAN2, DAN3 and DAN4. No such clear phase separation, however, was found in DAN5 due to its very weak temperature sensitivity.

When compared with the NIPAAm-DMAAm copolymer grafted dextran [7], most of the DAN series here appears to have a far more pronounced temperature-induced deswelling characteristic. For example, there was very little change of water content (93–96%) of the NIPAAm-DMAAm copolymer grafted dextran over a wide temperature of 25–45 °C, even though phase transition was observed from transparent to opaque. This lack of temperature-induced deswelling in the NIPAAm-DMAAm copolymer grafted dextran over its LCST occurred even with a high grafted NIPAAm-DMAAm copolymer content. Kumashiro *et al*. [7] speculated that the lack of intermolecular aggregation in the coil-globe transition might be responsible for the retention of high water content at a temperature greater than LCST.

Deswelling kinetics of the Dex-AI/PNIPAAm hybrid hydrogels

The data about the response kinetics of these hybrid hydrogels versus 100% PNIPAAm hydrogel are necessary for judging their potential in future applications. Generally, the slower response rate of the thermosensitive hydrogel is the greater restriction of its broad applications would be [40]. From the data in Fig. 11, we found that most of these Dex-AI/PNIPAAm hybrid hydrogels, except DAN5, had a faster deswelling response rate to the external temperature change than the 100% PNIPAAm hydrogel. For instance, DAN2 had its water retention reduced from 100% to nearly 35% within 5 min and 14% within 90 min, but the deswelling rate of a 100% PNIPAAm [41] was slower than most of DANs (DAN2, DAN3 and DAN4), but faster than DAN5. It is surprising to observe that, except DAN5, the incorporation of Dex-AI into PNIPAAm would result in a faster rate of deswelling of the hybrid hydrogels (DAN2-4) than the 100% PNIPAAm, even though the temperature sensitive component of the hybrid hydrogel (PNIPAAm) was diluted by the addition of the temperature-insensitive Dex-AI component. DAN5 was the only sample in the DAN hybrid series that had a

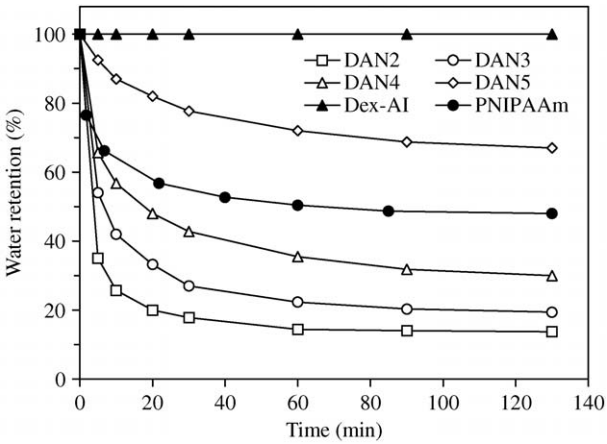

Figure 11 Temperature response kinetics of the Dex-AI/PNIPAAm hydrogels at 48 °C.

slower temperature-induced deswelling rate than the 100% PNIPAAm control (reducing to about 90 and 70% of the 100% PNIPAAm within the same time frame). Furthermore, during the deswelling kinetics study, it was noticed that only a few bubbles were observed on the skin layer of DAN2 and DAN3, while many bubbles appeared on the surface of DAN4 and DAN5. This correlation between deswelling rate and the composition ratio of the DAN hybrid series can be attributed to the wide range content of non-thermosensitive moiety (Dex-AI) in the DAN hybrids, which increased quickly from DAN2 to DAN5 (see Table I) as well as the difference in the crosslinking nature of Dex-AI from 100% PNIPAAm.

The deswelling process is a complicated process and many factors work together to control the hydrogel's response rate. If a thermosensitive, 3-D material could respond instantaneously to the external temperature change, and if the driven forces for collapsing in volume would result in the freeing and release of the entrapped water with minimum obstruction, this material would shrink dramatically in volume as temperature increases and a fast response rate would be achieved. However, if there would be any physical barrier to retard the release of the interior freed water during the collapsing of hydrogel network volume, the freed water would be forced to stay inside the material and interior pressure would be built up to such an extent to overcome the physical barrier and the freed water would then be released with the formation of water bubbles.

For a normal PNIPAAm hydrogel, when immersed into hot water at a temperature higher than its LCST, the outermost surface region of a PNIPAAm hydrogel shrinks first and rapidly, resulting in a thick and dense skin layer at the beginning of the shrinking process. This dense skin layer would act as a physical barrier for further water permeation and prevent the freed water to diffuse out from the interior hydrogel matrix. The relatively easier formation of dense outermost skin layer in 100% PNIPAAm hydrogel must be attributed to the use of a conventional crosslinking agent to tie PNIPAAm backbone chains together. Since the crosslinking could happen only at the two ends of a conventional crosslinking agent, the resulting 100% PNIPAAm hydrogel network is normally quite open, loose and porous with flexible cell wall as shown in Fig. 8. In the case of DAN hybrid series, the crosslinkable units (AI) were distributed along the dextran macromolecular backbone and hence provide far more extent of crosslinking than the 100% PNIPAAm system, that is, a more compact, dense, regular and rigid network structure (Fig. 8) and higher compression moduli (Fig. 5). Such unique pore structure and rigid cell wall may retard the formation of dense skin layer during the deswelling process over its LCST and hence better and faster release of freed water without the retardation effect from the dense surface layer than 100% PNIPAAm hydrogel [33, 42, 43]. So, the response rates of DAN2, DAN3 and DAN4 were faster than the 100% PNIPAAm hydrogel.

In addition to the capability of forming dense skin layer for controlling deswelling rate, the pore size of the network should also affect the response rate, and the larger pore size will lead to fast response rate [24, 25]. From this pore size standpoint, the response rate should decrease from DAN2 to DAN4 as we observed because their pore sizes decreased in this order.

Swelling kinetics of the Dex-AI/PNIPAAm hydrogels

Fig. 12 shows the effect of the composition ratio of the Dex-AI/PNIPAAm hybrid hydrogels on their water uptake rate at room temperature. The data show that all hybrid hydrogels exhibit significantly slower swelling rates than the normal PNIPAAm hydrogel; within the DAN hybrid series (except DAN5), as the content of Dex-AI in the hybrid hydrogels increased, the swelling or hydration rate of these hybrid hydrogels decreased. For example, the swelling ratio of the dried DAN2 reached 7.8 within 90 min, while that of DAN4 was 4.4 within the same time frame. Again, DAN5 shows an exception to this general composition dependence and is possibly attributed to its unique interior morphology shown in Fig. 8. The unique loose and large pore fishing net structure could allow water to diffuse into the inner matrix far more quickly than DAN3 and DAN4 could, that is, a higher rate of hydration than DAN3 and DAN4 as observed.

This dependence of hydration rate on the hybrid hydrogel composition is believed to be attributed to the different levels of crosslinking and polymer–polymer interactions, such as the hydrogen bonds and hydrophobic interactions. A swelling process of a hydrogel is controlled by three consecutive steps [44–46]: water molecules diffusion into the polymer system, the relaxation of the hydrated polymer chains and expansion of the polymer network into the aqueous solution. That is to say, during the reswelling process, strong inter/intramolecular interactions would greatly constrain the relaxation of the hydrated polymer chains, leading to a slower swelling or hydration rate for that hydrogel. Due to the unique crosslinking nature of the Dex-AI/PNIPAAm hybrid hydrogel as discussed above, the inter/intra-molecular interactions in the hybrid hydrogels were stronger than that in the 100% PNIPAAm hydrogel (evident in T_g and interior morphology). As a result, all the hybrid hydrogels exhibit slower swelling rates than

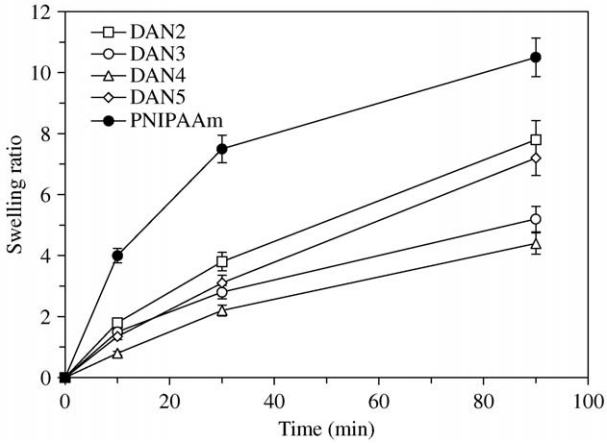

Figure 12 Reswelling kinetics of the vacuum dried Dex-AI/PNIPAAm hydrogels at 22 °C.

the 100% PNIPAAm control. Within the DAN hybrid series, due to the increase in the crosslinking from DAN2 to DAN4, the interactions among the polymeric network would be strengthened further and the three swelling steps would also become more difficult in the order from DAN2 to DAN4.

Conclusion

A novel class of partially biodegradable and thermosensitive hybrid hydrogels was synthesized by UV photocrosslinking the dextran-based precursor, Dex-AI, with the thermosensitive precursor, NIPAAm. The incorporation of the PNIPAAm segments into biodegradable Dex-AI would impart temperature stimulating capability to dextran system. However, the resulting hybrid hydrogels would have partial biodegradability that 100% PNIPAAm does not have.

The incorporation of Dex-AI into the PNIPAAm segments would not only increase LCST of the resulting hybrid hydrogels when comparing with the 100% PNIPAAm hydrogels, but also increase crosslinking level and result in a tighter and smaller pore network. Such a change in the interior morphology of hybrid hydrogels lead to the increase in the glass transition temperature with an increase in the Dex-AI content. Furthermore, when comparing with the 100% PNIPAAm hydrogel, these Dex-AI/PNIPAAm hybrid hydrogels also exhibited improved intelligent characterizations, such as the controllable response rate via changing the composition ratio of the precursors. In all, we demonstrated here a strategy to design and develop a new biodegradable and temperature sensitive hydrogel, which may find wide applications in many fields, such as biomedical and bioengineering fields.

Acknowledgments

We are grateful for the financial support of the National Textile Center (Project No.: M01-CR01).

References

1. Y. HIROKAWA and T. TANAKA, *J. Chem. Phys.* **81** (1984) 6379.
2. Y. G. TAKEI, T. AOKI, K. SANUI, N. OGATA, Y. SAKURAI and T. OKANO, *Macromolecules* **27** (1994) 6163.
3. X. Z. ZHANG and R. X. ZHUO, *Macromol. Chem. Physic.* **200** (1999) 2602.
4. B. JEONG, Y. H. BAE, D. S. LEE and S. W. KIM, *Nature* **388** (1997) 860.
5. B. JEONG, Y. H. BAE and S.W. KIM, *J. Contrl. Rel.* **63** (2000) 155.
6. B. JEONG, S. W. KIM and Y. H. BAE, *Adv. Drug. Delver. Rev.* **54** (2002) 37.
7. Y. KUMASHIRO, K. M. HUH, T. OOYA and N. YUI, *Biomacromolecules* **2** (2001) 874.
8. P. Y. P. KUO and W. M. SALTZMAN, *Crit. Rev. Eukaryotic. Gene Expr.* **6** (1996) 59.
9. Y. L. ZHANG and C. C. CHU, *ibid.* **59** (2002) 318.
10. S. H. KIM and C. C. CHU, *J. Biomater. Appl.* **15** (2000) 23.
11. Y. L. ZHANG and C. C. CHU, *ibid.* **16** (2002) 305.
12. C. Y. WON and C. C. CHU, *Carbohydr. Polym.* **36** (1998) 327.
13. Y. L. ZHANG, C. Y. WON and C. C. CHU, *J. Polym. Sci.: Polym. Chem.* **38** (2000) 2392.
14. J. CHEN, S. JO and K. PARK, *Carbohydr. Polym.* **28** (1995) 69.
15. L. D. TAYLOR and L. D. CERANKOWSKI, *J. Polym. Sci.: Polym. Chem. Ed.* **13** (1975) 2551.
16. X. P. QIU and C. WU, *Macromolecules* **30** (1997) 7921.
17. X. P. QIU, C. M. S. KWAN and C. WU, *ibid.* **30** (1997) 6090.
18. M. SHIBAYAMA, K. KAWAKUBO and T. NORISUYE, *ibid.* **31** (1998) 1608.
19. B. G. STUBBE, F. HORKAY, B. AMSDEN, W. E. HENNINK, S. C. DE SMEDT and J. DEMEESTER, *Biomacromolecules* **4** (2003) 691.
20. K. Z. GUMARGALIEVA, O. V. SHIPUNOVA, G. E. ZAIKOV, B. A. JUBANOV and S. A. MOSHKEVITCH, *Polym. Degrad. Stabil.* **51** (1996) 57.
21. W. N. E. VAN DIJK-WOLTHUIS, J. A. M. HOOGEBOOM, M. J. VAN STEENBERGEN, S. K. Y. TSANG and W. E. HENNINK, *Macromolecules* **30** (1997) 4639.
22. O. FRANSSEN, R. D. VAN OOIJEN, D. DE BOER, R. A. A. MAES and W. E. HENNINK, *ibid.* **32** (1999) 2896.
23. C. J. DE GROOT, M. J. A. VAN LUYN, W. N. E. VAN DIJK-WOLTHUIS, J. A. CADÉE, J. A. PLANTINGA, W. DEN OTTER and W. E. HENNINK, *Biomaterials* **22** (2001) 1197.
24. Y. L. ZHANG and C. C. CHU, *J. Mater. Sci.: Mater. M.* **13** (2002) 667.
25. X. Z. ZHANG, Y. Y. YANG, T. S. CHUNG and K. X. MA, *Langmuir* **17** (2001) 6094.
26. X. Z. ZHANG, Y. Y. YANG and T. S. CHUNG, *J. Colloid Interf. Sci.* **246** (2002) 105.
27. H. INOMATO, S. GOTO and S. SAITO, *Macromolecules* **23** (1990) 4887.
28. H. FEIL, Y. H. BAE, J. FEIJEN and S. W. KIM, *ibid.* **26** (1993) 2496.
29. T. TOKUHIRO, T. AMIYA, A. MAMADA and T. TANAKA, *ibid.* **24** (1991) 2936.
30. G. BOKIAS, D. HOURDET, I. ILIOPOULOS, G. STAIKOS and R. AUDEBERT, *ibid.* **30** (1997) 8293.
31. B. VERNON, S. W. KIM and Y. H. BAE, *J. Biomed. Mater. Res.* **51** (2000) 69.
32. M. SHIBAYAMA, Y. FUJIKAWA and S. NOMURA, *Macromolecules* **29** (1996) 6535.
33. E. S. MATSUO and T. TANAKA, *J. Chem. Phys.* **89** (1988) 1695.
34. X. Z. ZHANG and R. X. ZHUO, *Langmuir* **17** (2001) 12.
35. X. Z. ZHANG, D. Q. WU and C. C. CHU, *J. Polym. Sci.: B Polym. Phys.* **41** (2003) 582.
36. R. G. SOUSA, W. F. MAGALHAES and R. F. S. FREITAS, *Polym. Deg. Stab.* **61** (1998) 275.
37. E. DIEZ-PENA, I. QUIJADA-GARRIDO, P. FRUTOS and J. M. BARRALES-RIENDA, *Macromolecules* **35** (2002) 2667.
38. Y. L. ZHANG and C. C. CHU, *J. Mater. Sci.: Mater. M.* **13** (2002) 773.
39. X. Z. ZHANG, Y. Y. YANG, F. J. WANG and T. S. CHUNG, *Langmuir* **18** (2002) 2013.
40. J. KOPECEK, *Nature* **417** (2002) 388.
41. X. Z. ZHANG, R. X. ZHUO and Y. Y. YANG, *Biomaterials* **23** (2002) 1313.
42. Y. H. BAE, T. OKANO and S. W. KIM, *Makromol. Chem. Rapid. Commun.* **9** (1988) 185.
43. Y. KANEKO, K. SAKAI, A. KIKUCHI, R.YOSHIDA, Y. SAKURAI and T. OKANO, *Macromolecules* **28** (1995) 7717.
44. R. YOSHIDA, Y. OKUYAMA, K. SAKAI, T. OKANO and Y. SAKURAI, *J. Membr. Sci.* **89** (1994) 267.
45. D. J. ENSCORE, H. B. HOPFRNBERG and V. T. STANNETT, *Polymer* **18** (1977) 793.
46. X. Z. ZHANG and R. X. ZHUO, *J. Colloid Interf. Sci.* **223** (2000) 311.

Received 23 June 2003
and accepted 10 February 2004